Mon. Not. R. Astron. Soc. **303,** 65–76 (1999)

Fundamental parameters of the moderately young open clusters NGC 5999, NGC 6031, Ruprecht 115 and Ruprecht 120

Andrés E. Piatti,[1]★†‡ Juan J. Clariá[1] and Eduardo Bica[2]
[1]*Observatorio Astronómico, Laprida 854, 5000 Córdoba, Argentina*
[2]*Universidade Federal do Rio Grande do Sul, Departamento de Astronomía, CP 15051, Porto Alegre, 91500-970, Brazil*

Accepted 1998 October 5. Received 1998 September 28; in original form 1998 June 4

ABSTRACT

We present CCD *BVI* Johnson–Cousins photometry for the southern open clusters NGC 5999, NGC 6031, Ruprecht 115 and Ruprecht 120. The sample consists of about 1160 stars reaching down to $V \sim 19$ mag. From the analysis of the colour–magnitude diagrams, we confirm the reality of the clusters and derive their fundamental parameters (reddening, distance and age). We also present integrated spectra for NGC 6031, Ruprecht 115 and Ruprecht 120, covering a range from 3500 to 9200 Å. From the equivalent widths of Balmer and infrared Ca II triplet lines, as well as from a comparison of the obtained spectra with those of template clusters, we derive reddening, age and metallicity. The photometric and spectroscopic results allow us to conclude that the four clusters are moderately young (age ~100–500 Myr) and are located approximately towards the Galactic Centre at ~2.3 kpc from the Sun. NGC 6031 and Ruprecht 120 have nearly solar metal content, while Ruprecht 115 appears to be slightly metal-rich.

Key words: methods: observational – open clusters and associations: general – open clusters and associations: individual: NGC 5999 – open clusters and associations: individual: NGC 6031 – open clusters and associations: individual: Ruprecht 115 – open clusters and associations: individual: Ruprecht 120.

1 INTRODUCTION

Open clusters have long been recognized as important tools in the study of the Galactic disc. Old and intermediate-age open clusters are excellent probes of early disc evolution, while young open clusters provide information about current star formation processes and are key objects to delineate Galactic structure. Galactic open clusters of small angular size are also fundamental as calibrators of integrated properties in view of population synthesis studies in galaxies (see, e.g., Bica & Alloin 1986a, 1987, hereafter BA86a, BA87) and the determination of astrophysical parameters of star clusters in distant galaxies for which it is not possible to obtain colour–magnitude diagrams (CMDs).

The present study is part of an ongoing project of observation of open cluster candidates mostly located in the direction of the Galactic Centre (Piatti 1996; Piatti, Bica & Clariá 1998a; Piatti et al. 1998b). The main purpose of this long-term programme is to obtain CCD photometric and integrated spectroscopic data of southern open cluster candidates not yet observed or with incomplete observations, in order to determine whether they are genuine physical systems or if, on the contrary, the apparent concentration of stars in a sky region is a consequence of random fluctuations of the stellar density in that zone. The photometric and spectroscopic data allow a detailed study of those objects confirmed as open clusters and therefore to improve our knowledge of their fundamental parameters. By enlarging the sample of well-studied open clusters in the direction of the Galactic Centre, we can address the question of the structure and chemical evolution of the inner Galactic disc.

Although new open clusters towards the Galactic Centre were detected during the last decade (see, e.g., Janes & Phelps 1990), few of them have been studied in detail. With the advent of the CCD detectors, we can obtain more and better information about open clusters. The precision of the CCD photometry is significantly higher than that of the photographic photometry, generally used in large-scale cluster studies. By using CCD photometry, it is possible to derive basic properties from very compact clusters, which would

★Visiting Astronomer, Complejo Astronómico El Leoncito, which is operated under agreement between the Consejo Nacional de Investigaciones Científicas y Técnicas de la República Argentina and the National Universities of La Plata, Córdoba, and San Juan, Argentina.
†Visiting Astronomer, University of Toronto (David Dunlap Observatory) 24-inch telescope, Las Campanas, Chile.
‡Visiting Astronomer, Cerro Tololo Inter-American Observatory, National Optical Astronomy Observatories, operated by the Association of Universities for Research in Astronomy, Inc., under contract with the National Science Foundation.

Table 1. Journal of observations.

Object	Date (UT)	Photometric data Filter	Exposures	FWHM (″)
NGC 5999	1994 September 4	B	1×60 s, 2×300 s	1.3
		V	1×60 s, 2×150 s	1.3
		I	1×20 s, 2×60 s	1.3
NGC 6031	1994 September 3	B	1×60, 300, 400 s	1.4
		V	1×60, 250, 300 s	1.4
		I	1×15, 40, 70 s	1.4
Ruprecht 115	1995 June 29	B	1×60 s, 2×600 s	1.5
		V	1×60 s, 2×300 s	1.4
		I	1×15 s, 2×30 s	1.5
Ruprecht 120	1995 July 2	B	1×60 s, 2×900 s	1.4
		V	1×60 s, 2×600 s	1.4
		I	1×30 s, 2×120 s	1.4
		Spectroscopic data		
Object	Date (UT)	Spectral range	Exposures	FWHM (″)
NGC 6031	1995 May 20	blue	4×900 s	2.2
	1995 May 23	red	4×900 s	2.3
Ruprecht 115	1995 May 27	blue	4×900 s	2.1
	1995 May 28	red	4×900 s	2.2
Ruprecht 120	1995 May 27	blue	4×900 s	2.1
	1995 May 29	red	4×900 s	2.0

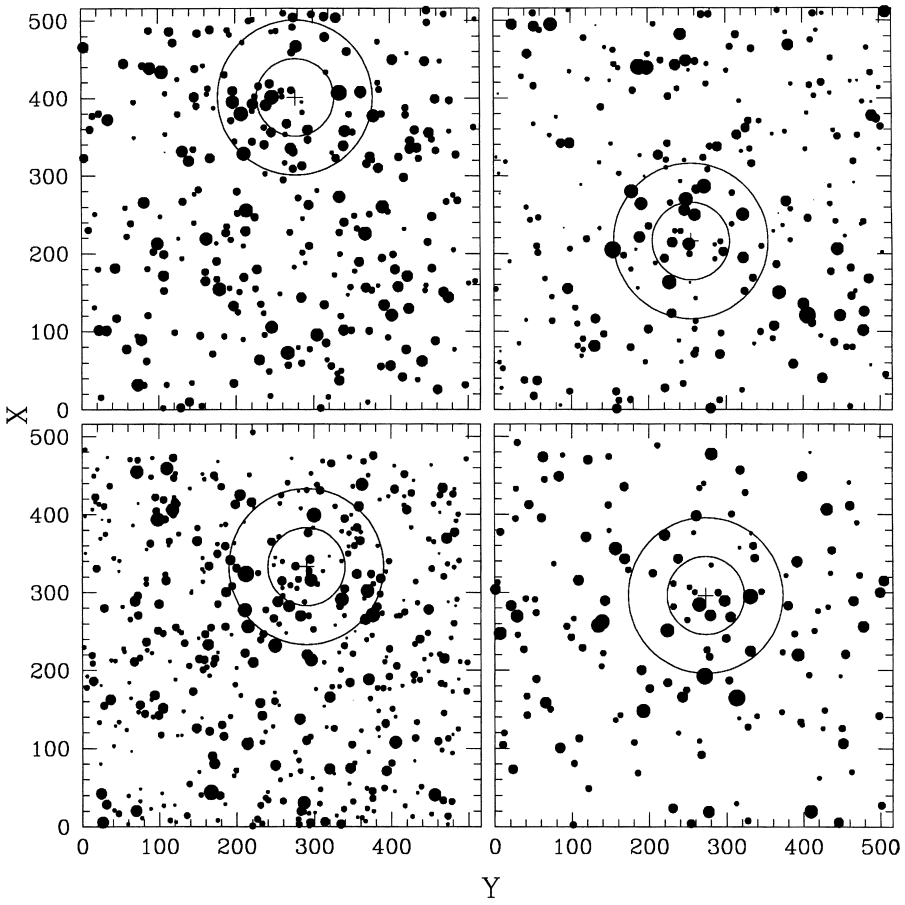

Figure 1. Schematic finding charts for the fields of NGC 5999 (top-left), NGC 6031 (top-right), Ruprecht 115 (bottom-left), and Ruprecht 120 (bottom-right). A cross indicates the adopted cluster centre. Two concentric circles of 22.5- and 45.0-arcsec radii are also shown. North is up and east is to the left.

Table 2. Transformation coefficients.

Date (UT)	b_1	b_2	v_1	v_2	i_1	i_2
1994 September 3	6.357	−0.016	6.027	−0.040	5.283	−0.039
	±0.012	±0.006	±0.007	±0.005	±0.013	±0.007
1994 September 4	6.300	−0.017	5.920	−0.052	5.230	−0.055
	±0.011	±0.007	±0.010	±0.008	±0.010	±0.010
1995 June 29	7.267	−0.043	7.051	−0.039	6.551	−0.084
	±0.009	±0.004	±0.009	±0.010	±0.011	±0.011
1995 July 2	7.210	−0.044	6.974	−0.039	6.563	−0.075
	±0.010	±0.005	±0.008	±0.004	±0.012	±0.007

be practically impossible with traditional techniques. Moreover, many open clusters formerly observed with photographic or even photoelectric techniques have been reobserved with CCD detectors, resulting in better CMDs and, hence, more precise fundamental parameters (see, e.g., Montgomery, Marschall & Janes 1993 and Daniel et al. 1994).

CCD integrated spectra of small objects, from which it is very difficult to obtain individual information about stars unaffected by contamination, are fundamental not only to recognize the nature of objects such as galaxies, nebulae, stellar clusters, supernova remnants, etc. (see, e.g., Bica et al. 1995), but also to determine the reddening, age and metallicity of open clusters (see, e.g., Santos & Bica 1993; Bica et al. 1998 and Piatti et al. 1998a, 1998b).

We report here the results of the first CCD observation campaigns for the poorly studied or unstudied southern open clusters NGC 5999 ($\alpha_{1950} = 15^{\rm h}48^{\rm m}.2$, $\delta_{1950} = -56°19'$; $l = 326°.02$, $b = -1°.93$), NGC 6031 ($\alpha_{1950} = 16^{\rm h}03^{\rm m}.7$, $\delta_{1950} = -53°56'$; $l = 329°.25$, $b = -1°.53$), Ruprecht 115 ($\alpha_{1950} = 16^{\rm h}09^{\rm m}.0$, $\delta_{1950} = -52°15'$; $l = 330°.97$, $b = -0°.83$) and Ruprecht 120 ($\alpha_{1950} = 16^{\rm h}31^{\rm m}.7$, $\delta_{1950} = -48°12'$; $l = 336°.40$, $b = -0°.54$). The published data on these clusters is rather heterogeneous. NGC 6031 is the only cluster in the sample with several previous studies. Although old cataloguing works assign to this object distances ranging between 1.7 and 7.7 kpc (Trumpler 1930; Collinder 1931; Barkhatova 1960), more recent determinations place it approximately at 2.0 kpc from the Sun (Lindoff 1967; Moffat & Vogt 1975, hereafter MV75; Fenkart & Binggeli 1979; Topaktas 1981). With the exception of the study by MV75, based on *UBV* photoelectric photometry of 16 stars, most of the works are based on photographic observations. A comparison between the results obtained by MV75 and Topaktas (1981) shows that the differences in the fits of the zero-age-main-sequence (ZAMS), regardless of the observational errors, reach $\Delta M_v \approx 1.0$ mag, which in turn leads to a difference in the distance determination of 1.2–1.7 kpc. MV75 also suggest that the difference of 2.1 kpc found between their distance estimation and that of Lindoff (1967) may be caused by errors inherent to Lindoff's photographic photometry. However, the main source of error in the distance modulus would appear to be the intrinsic dispersion observed in the sequence of NGC 6031.

No photometric studies are available for NGC 5999, Ruprecht 115 or Ruprecht 120, while spectroscopic data are available only for NGC 5999. Santos & Bica (1993) obtained an integrated spectrum of NGC 5999 and derived a foreground reddening of $E(B-V)_{\rm f} = 0.44$ and an age of 100 Myr from the matching between the spectrum of NGC 5999 and template spectra. They also estimated a slightly greater age ($t \sim 230$ Myr) from Balmer lines, and a metallicity of [Fe/H] = 0.18 from Ca II triplet lines. The four studied clusters have small angular diameters which make them ideal for CCD camera analysis.

In the next section we describe the CCD *BVI* photometric and integrated spectroscopic observations and their calibrations. We also present *UBV* photoelectric measurements of 27 stars in the field of NGC 5999. In Section 3.1 we present the observed (V, $B-V$) and (V, $V-I$) diagrams and discuss their properties. In Section 3.2 we analyse the CCD integrated spectra. Section 4 summarizes the main conclusions of this study.

2 OBSERVATIONS AND REDUCTIONS

BVI Johnson–Cousins images were obtained by using the 24-inch telescope of the University of Toronto Southern Observatory at Las Campanas, Chile, in 1994 September and 1995 June-July. A PM 512×512 METACHROME CCD, which was coated to give improved blue response, was employed in both runs. The scale on the chip was 0.45 arcsec per pixel, resulting in a CCD field of about 4×4 arcmin^2. Four Selected Area standard fields of Landolt (1992) were observed nightly (40 stars in total, with an average of 14 standards per night). All the nights were photometric, with a typical seeing of 1.4 arcsec. A series of 10 bias exposures and 10 flat-field frames on the illuminated dome and twilight sky were obtained for each night. Table 1 summarizes the observations, while Fig. 1 shows schematic finding charts of the observed cluster fields. The airmass values for both the observed and standard fields range between 1.08 and 1.34.

The observations were reduced at the Astronomical Observatory of Córdoba, Argentina, using the IRAF[1] software package in the standard way. The images were bias-subtracted and flat-fielded by employing weighed combined signal-calibrator frames. In addition, we checked for the existence of any illumination pattern on the chip; no correction was necessary. Then, the instrumental magnitudes for the standard and programme fields were derived from aperture photometry and point spread function fits under DAOPHOT/IRAF routines (Stetson 1991), respectively. Atmospheric extinction was removed with the coefficients from Vázquez et al. (1996). The equations used to transform the b, v and i instrumental magnitudes into the V, $(B-V)$ and $(V-I)$ standard magnitudes and colours are the following:

$$b_{j,n} = b_1 + V + (B-V) + b_2(B-V), \quad (1)$$

$$v_{k,n} = v_1 + V + v_2(B-V), \quad (2)$$

$$i_{l,n} = i_1 + V - (V-I) + i_2(V-I). \quad (3)$$

Note that for each night n there are as many instrumental magnitudes per filter as observed standard stars, so that equations (1) to (3)

[1] IRAF is distributed by the National Optical Astronomy Observatories, which is operated by the Association of Universities for Research in Astronomy, Inc., under contract to the National Science Foundation.

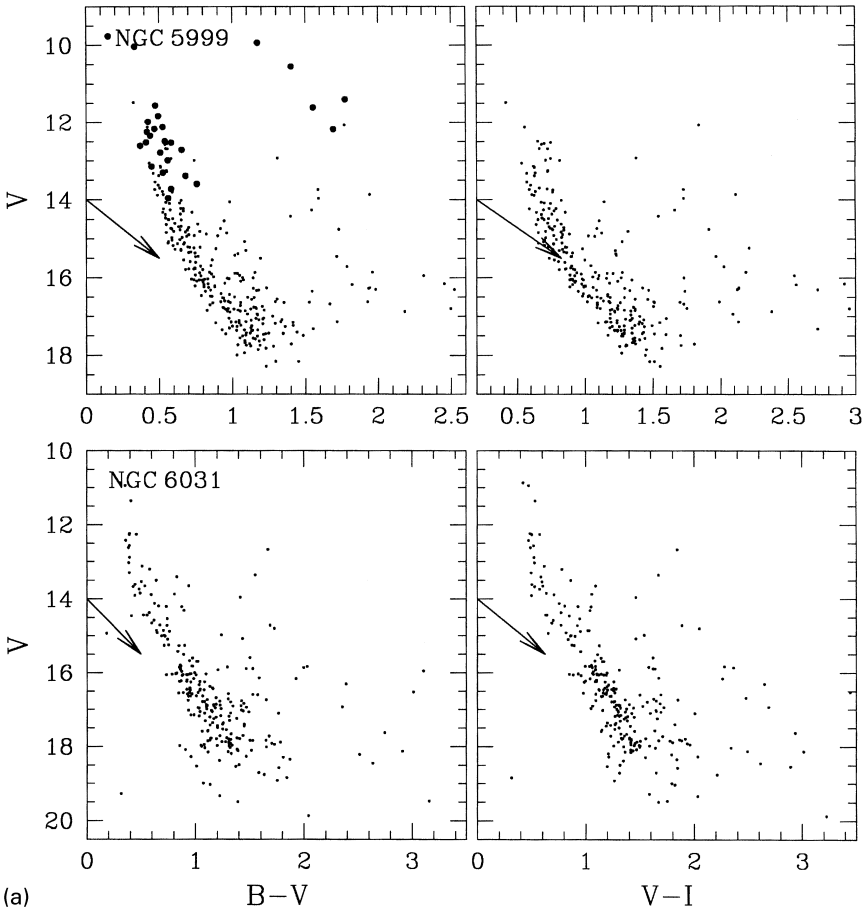

Figure 2. (a) (V, $B-V$) and (V, $V-I$) diagrams of stars in the fields of NGC 5999 (top) and NGC 6031 (bottom).

were fitted by least-squares simultaneously. The rms errors affecting the calibrations of equations (1), (2) and (3) are 0.010, 0.009 and 0.011, respectively, whereas the resulting coefficient values are listed in Table 2. Next, we obtained three independent tables for each programme field containing the V, $(B-V)$ and $(V-I)$ magnitudes and colours for all the measured stars, together with the corresponding X and Y coordinates and the photometric errors as deduced from the INVERFITS/IRAF task. Finally, the different tables were cross-correlated in order to improve the statistics for stars with two or three independent measurements. This procedure allowed us to obtain the individual photometric internal errors as well as to detect any anomalous value. A comparison between our observations and those of MV75 for 15 stars in NGC 6031 yields $V_{\rm MV75}-V_{\rm CCD}=-0.023\pm0.035$ and $(B-V)_{\rm MV75}-(B-V)_{\rm CCD}=-0.001\pm0.022$, which show that there are no significant offsets in our CCD zero-point magnitude and colour scales.

We also carried out photoelectric BV measurements of 27 bright stars within a field of 15×15 arcmin^2 centred on NGC 5999. The observations were performed during four photometric nights in 1994 April with the 0.6- and 1.0-m telescopes at Cerro Tololo Inter-American Observatory (CTIO) and the PC/ASCAP data aquisition software. A dry-ice cooled Hamamatsu R943-02 photomutiplier was used with pulse-counting equipment. Mean extinction coefficients were determined for each night. The BV standard system was established by nightly observing between 12 and 17 standard stars from the lists of Landolt (1973) and Graham (1982). The reductions were similar to those quoted in previous papers (e.g. Clariá & Lapasset 1991), and the resulting external mean errors are $\sigma_V=0.008$ and $\sigma_{B-V}=0.010$. A comparison between the present CCD and photoelectric BV data for five stars in common yields $V_{\rm pe}-V_{\rm CCD}=-0.020\pm0.017$ and $(B-V)_{\rm pe}-(B-V)_{\rm CCD}=0.011\pm0.009$, which shows an excellent agreement.

The integrated spectroscopic observations were carried out with the 2.15-m telescope at the Complejo Astronómico El Leoncito (CASLEO, Argentina) during a run in 1995 May. We employed a REOSC spectrograph containing a Tektronics CCD of 1024×1024 pixels, the size of each pixel being 24×24 μm^2. All the integrated spectra were obtained by scanning the slit across the cluster. The total field along the slit was 4.7 arcmin and, consequently, we could sample background regions. A 300 line mm^{-1} grating was used in two different set-ups, namely 'blue nights' and 'red nights'. During the blue nights, we obtained spectra ranging from 3500 to 7000 Å, with an average dispersion in the observed region of 140 Å mm^{-1} (3.46 Å pixel^{-1}). The slit width was 4.2 arcsec, resulting in an average resolution of 14 Å, according to the FWHM of the He-Ar comparison lamps. During the red nights, we obtained spectra from 5800 to 9200 Å, with a similar dispersion (3.36 Å pixel^{-1}) and a resolution of 17 Å (same slit width). Besides, to eliminate second-order contamination, an OG 550 filter was employed. Exposures of 15 min each were performed for NGC 6031, Ruprecht 115 and Ruprecht 120, with a total of one hour for the blue and red spectra. We did not carry out observations for NGC 5999 because its

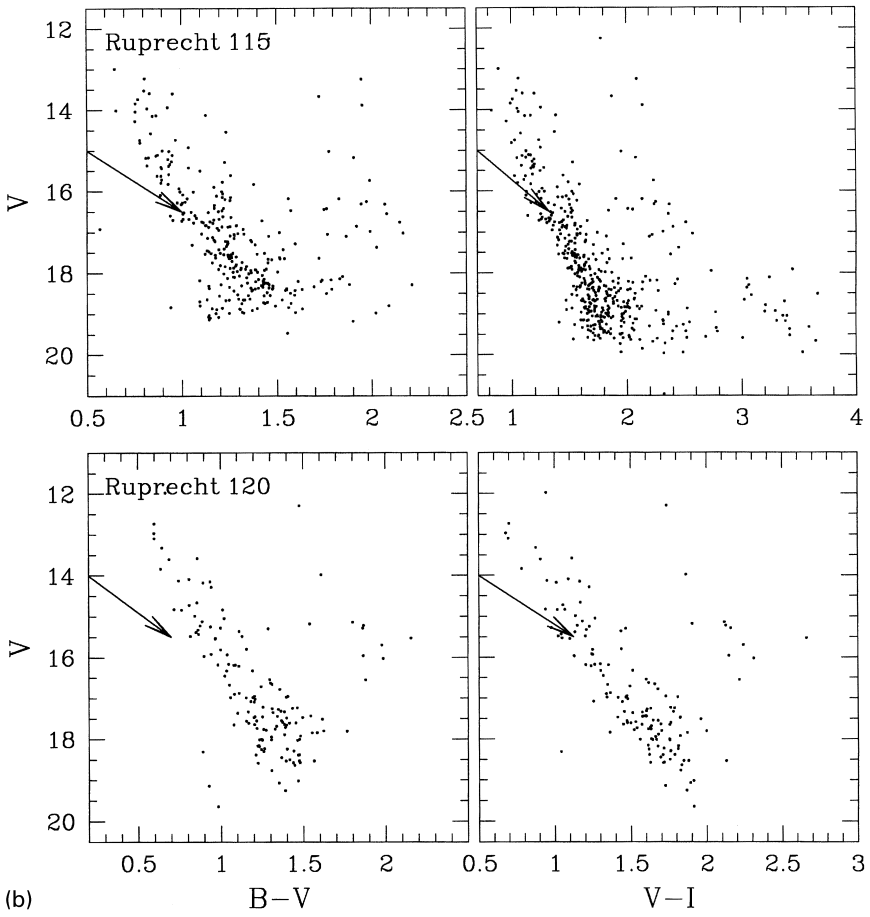

Figure 2. (b) $(V, B-V)$ and $(V, V-I)$ diagrams of stars in the fields of Ruprecht 115 (top) and Ruprecht 120 (bottom).

integrated spectrum had been previously obtained by Santos & Bica (1993). Table 1 includes the log for the spectroscopic observations. We also observed spectrophotometric standards to derive flux calibrations. Stars LTT 4364, EG 274 and LTT 7379 (Stone & Baldwin 1983) were used in the blue range. In the red range, the hot dwarf star HD 160233 (Gutiérrez-Moreno et al. 1988) was added to the standard list, which allowed us the correction for telluric absorption bands. Frames of He-Ar comparison lamps between and after the object observations, bias and dome, twilight sky, and tungsten lamp flat-fields were also taken. The integrated spectra were reduced at the Astronomical Observatory of Córdoba, following the precepts described by Piatti et al. (1998a). Finally, we eliminated the telluric absorption bands in the near-IR, following the procedures outlined in BA87.

3 ANALYSIS AND DISCUSSION

3.1 Photometric data

The presence in the sky of a star concentration does not necessarily imply the existence of a physical system. To confirm the physical reality of such system, astrometric and kinematic information as well as photometric data are required. However, due to the fact that the number of open clusters with known proper motions and radial velocities is much smaller than the number of clusters observed photometrically, the photometric information often constitutes the only available tool to infer the existence of an open cluster.

We have plotted in Figs 2(a) and (b) the $(V, B-V)$ and $(V, V-I)$ CMDs for all the measured stars in NGC 5999, NGC 6031, Ruprecht 115 and Ruprecht 120. Stars observed photoelectrically in NGC 5999 are represented with filled circles in Fig. 2(a). All the CMDs reveal clear star sequences with relatively little field star contamination. It is difficult to separate field stars from the cluster members only on the basis of their closeness to the main populated area of the CMDs, because field stars at the cluster distance and reddening will also occupy this area. However, the possibility of cluster membership is small for the stars located well away from the main sequences (MSs) in Figs 2(a) and (b). The most poorly defined star sequences correspond to Ruprecht 120, whereas the $(V, V-I)$ diagram of Ruprecht 115 is nearly 1 mag deeper than that based on the $B-V$ colour. Note also that the $(V, B-V)$ diagram of NGC 6031 contains stars in the sequence almost 3 mag fainter than those observed in previous photographic studies (e.g. Lindoff 1967; Topaktas 1981).

The argument that the stars observed in some limited region of the sky show a general appearance in the CMD rather similar to a MS is frequently explicity or implicity presented as evidence of the physical reality of a cluster. However, field stars can also show the appearance of a sequence in the CMDs, its morphology being different from that of an open cluster MS. Burki & Maeder (1973) showed that field dwarf sequences have a lower envelope, which does not depend on the space density of stars, but on the parameters of interstellar extinction, namely $R = A_v/E(B-V)$. They also found that these sequences have a curvature smaller than that of

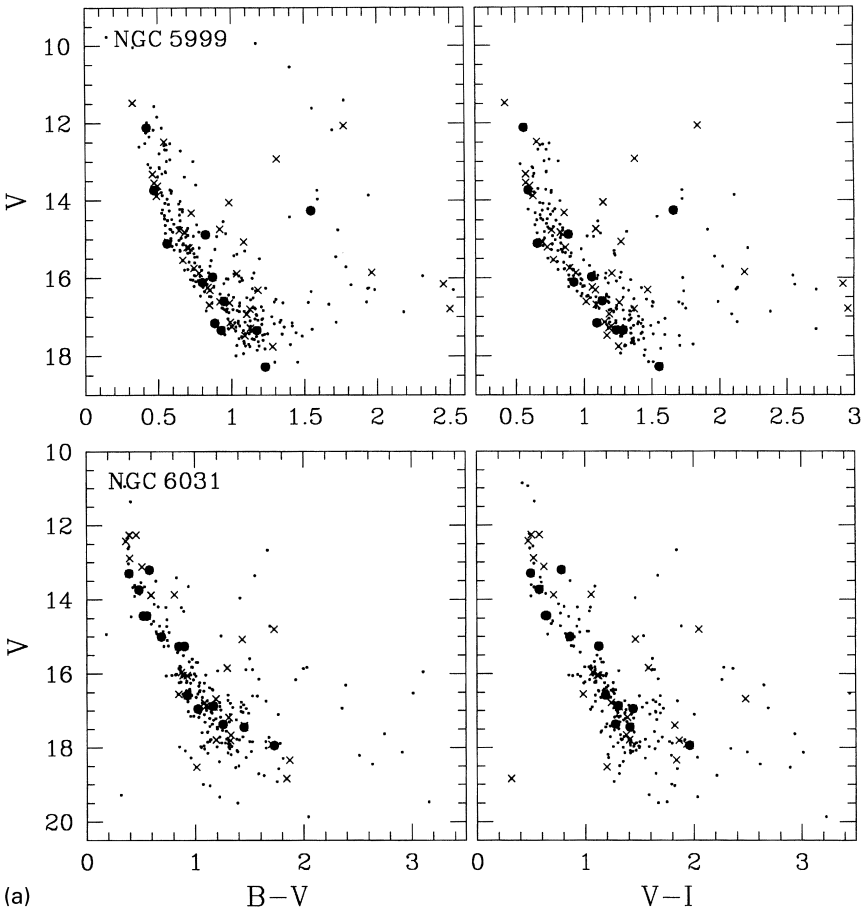

Figure 3. (a) Colour–magnitude diagrams of stars in the field of NGC 5999 (top) and NGC 6031 (bottom): all measured stars (dots), circular extraction for $r < 22.5$ arcsec (filled circles) and $r < 45.0$ arcsec (crosses) are superimposed.

the ZAMS. On the other hand, a field-star sequence parallel to the reddening vector could arise if (a) the stars were at almost exactly the same distance, (b) the stars were of very similar spectral classes, (c) the stars were subject to differing amounts of reddening, or (d) these three conditions were combined. The lines drawn to the left of the sequences in Figs 2(a) and (b) indicate the direction of the reddening vectors in each CMD. The size of these vectors correspond to an $E(B-V)$ colour excess of 0.5 mag, assuming $A_v = 3.0E(B-V)$ and $E(V-I) = 1.25E(B-V)$, respectively. Hence we confirm that the observed star sequences appear to be MSs of moderately young open clusters.

Ng et al. (1996) have recently studied the contribution of stars from the disc population to CMDs of star fields located at low galactic latitudes in the direction of the Galactic Centre. They have also identified the regions of the CMDs where the disc stars are located. According to these findings, the sequence of red stars at about $(V-I) \sim 3.4$ in the $(V, V-I)$ diagram of Ruprecht 115 should correspond to evolved stars of an intermediate-age/old disc population component. Note that this sequence has a slope quite similar to that of the reddening vector.

Although the four observed objects resemble genuine open clusters, there are some features in the CMDs which deserve an additional analysis before determining the clusters fundamental parameters. It would be interesting, for example, to define fiducial MSs by avoiding possible non-physical members. In fact, the broadness of the MSs may be either an intrinsic characteristic of the clusters or one caused by field star contamination and/or by variable reddening. Note also that the observed colours of the turn-offs suggest that the clusters should be affected by relatively high reddening. In this sense, particular attention should be paid to the stars distributed very close to the most populated region of the cluster MSs.

To obtain the CMDs of the cluster core regions, we first determined the cluster centres and then carried out extractions of the stars distributed within 50 (22.5 arcsec) and 100 (45.0 arcsec) pixels wide annuli, respectively. This was accomplished by building the stellar density profiles as a function of pixel bins in the x and y directions, using all the stars of Figs 2(a) and (b). The adopted final coordinates for the cluster centres are $(X_c, Y_c) = (401, 277)$, (216, 255), (333, 290) and (296, 273) for NGC 5999, NGC 6031, Ruprecht 115 and Ruprecht 120, respectively. The resulting extracted CMDs are shown in Figs 3(a) and (b). Stars located within 50- and 100-pixel wide annuli (see Fig. 1) are shown as filled circles and crosses, respectively, whereas dots represent the remaining stars. An inspection of Figs 3(a) and (b) reveals that the cluster MSs are, in general, tighter than the observed sequences. Note, for example, that the apparent star sequence parallel to the MS of Ruprecht 120 is formed mostly by field stars and not by possible cluster binary stars, as might be expected. Small star clumps near the MS of NGC 6031 and Ruprecht 115 are also field stars.

In order to estimate the mean cluster reddening and apparent distance modulus, we matched the extracted $(V, B-V)$ and

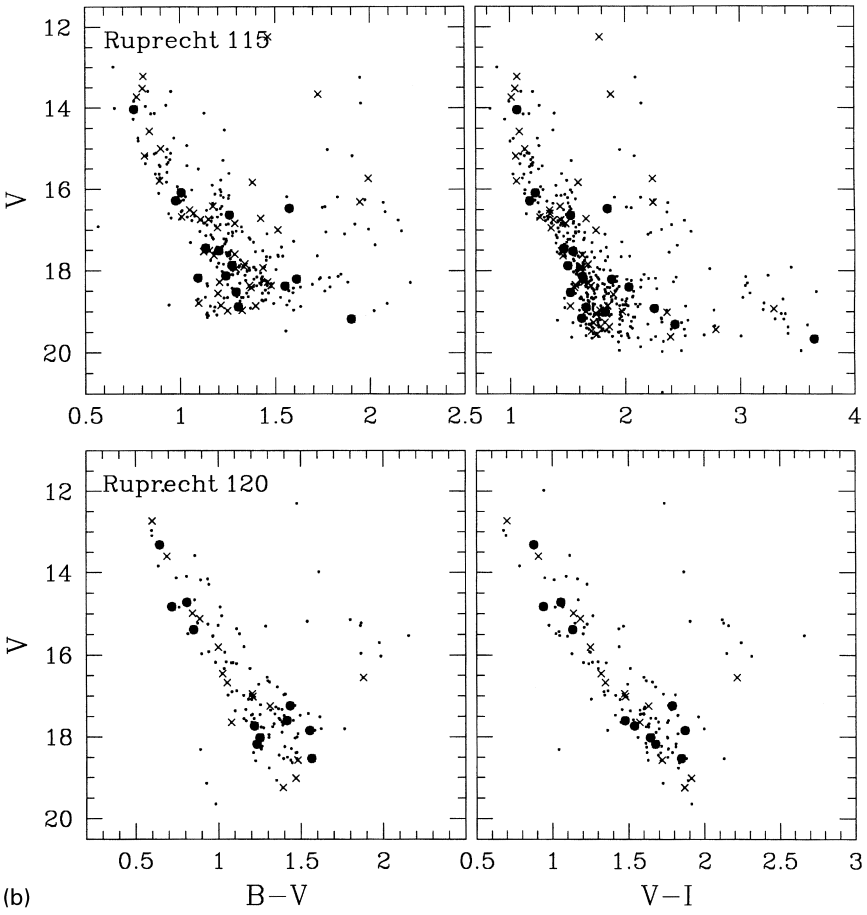

Figure 3. (b) Colour–magnitude diagrams of stars in the fields of Ruprecht 115 (top) and Ruprecht 120 (bottom): symbols same as in (a).

Table 3. Cluster fundamental parameters derived from the CMDs analysis.

Cluster	$E(B-V)$	$E(V-I)$	$V-M_v$	Age (Myr)	σ (Myr)
NGC 5999	0.45	0.55	13.00	400	100
NGC 6031	0.50	0.55	12.75	250	100
Ruprecht 115	0.65	0.90	13.75	600	100
Ruprecht 120	0.70	0.95	13.75	150	100

(V, $V-I$) diagrams to the ZAMSs of Schmidt-Kaler (1982) and Piatti, Clariá & Bica (1998c), respectively. Considering that it is possible to change reddening and distance modulus simultaneously, and even obtain a satisfactory fitting, we decided to use as reference the $E(B-V)$ colour excesses and ages provided by the spectroscopic analysis (see Section 3.2). The resulting $E(B-V)$ and $E(V-I)$ colour excesses and apparent distance moduli are listed in Table 3. The errors affecting these quantities as estimated from the fitting are 0.05, 0.05 and 0.25, respectively. Note that these errors reflect only the dispersion around the adopted mean values. On the other hand, we derived a mean value for the ratio $E(V-I)/E(B-V) = 1.27 \pm 0.11$, which indicates that the interstellar absorption towards the clusters follows approximately the normal extinction law. In the subsequent analysis, we have therefore adopted the values 1.25 and 3.0 for the $E(V-I)/E(B-V)$ and $R = A_v/E(B-V)$ ratios, respectively (Turner 1976; Walker 1985; Straižys 1990).

We have estimated cluster ages by using the empirical isochrones recently published by Piatti et al. (1998c). These isochrones, obtained from high-quality CCD *VI* data of template open clusters spanning a wide age range, are useful for deriving ages of highly reddened open clusters regardless of their metallicity, since $(V-I)_o$ is virtually free from metallicity effects (e.g. Rosvick 1995; Kassis, Friel & Phelps 1996). We first applied reddening and distance corrections to the observed CMDs using the $E(V-I)$ and $V-M_v$ values listed in Table 3, and then fitted the empirical isochrones to the cluster M_v versus $(V-I)_o$ diagrams and interpolated values between them. The ages were estimated from the MS stars distributed within 100-pixel wide annuli in each cluster. The resulting values are listed in column 5 of Table 3, whereas Fig. 4 shows the M_v versus $(V-I)_o$ diagrams with the isochrones superimposed. Open circles and boxes in Fig. 4 represent the loci of the red giant clumps of the template open clusters NGC 6067 (age 160 Myr; Meynet, Mermilliod & Maeder 1993) and NGC 6259 (age = 200 Myr; Hawarden 1974, Meynet et al. 1993), respectively.

3.2 Spectroscopic data

Fig. 5 illustrates the obtained integrated spectra for NGC 6031, Ruprecht 115 and Ruprecht 120, normalized to $F_\lambda = 1$ at $\lambda = 6000$ Å. The S/N ratios of these spectra – measured at the same continuum region – have a typical value of 30, which allows us to distinguish spectral absorption features differing by around 10 per cent of the continuum intensity, i.e., with residual intensities

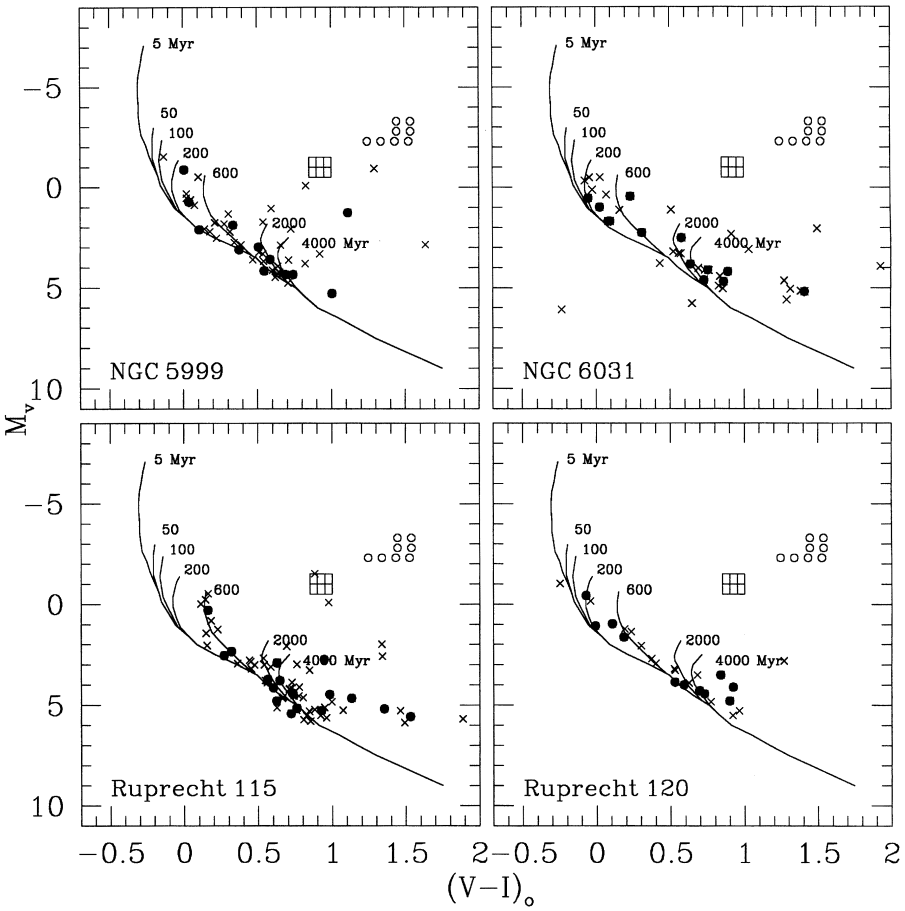

Figure 4. M_v versus $(V-I)_o$ diagrams with the isochrones of Piatti et al. (1998) superimposed. Only stars corresponding to the circular extractions are drawn. Symbols are as in Fig. 3.

higher than 90 per cent of the continuum flux. On the other hand, the slopes of the continuum energy distributions are the result of combined reddening and age effects. The spectrum of Ruprecht 120, for instance, is essentially flat towards longer wavelengths, in contrast with the negative slope of the spectrum of the slightly older cluster NGC 6031. This difference is mainly due to reddening effects. At the same time, evolutionary effects produce nearly similar continuum energy distributions in the spectra of Ruprecht 115 and 120. These two clusters have approximately the same $E(B-V)$ colour excess, the former being older by a factor of 5 (see Section 3.1).

The determination of the fundamental cluster parameters from their integrated spectra was carried out by using the SPEED spectral analysis software (Schmidt 1988) at the Astronomical Observatory of Córdoba. BA86a and BA87 examined the behaviour of metallic and Balmer-line equivalent widths as well as the continuum energy distribution in the spectral range 3700–10 000 Å from integrated spectra of Galactic and Magellanic Cloud star clusters. They also generated a library of template cluster spectra with well-known properties. To determine the fundamental cluster parameters, we applied the procedures described by BA86a and BA87. A direct reddening-independent age estimate was first obtained from equivalent widths of the Balmer lines in absorption in each spectrum by interpolating these values into the age calibration of Bica & Alloin (1986b, hereafter BA86b). Using this first age estimate, we selected an appropriate set of template spectra and derived cluster reddening by matching each observed spectrum to that of the template which most resembled it.

The equivalent widths of the Balmer lines were measured, taking into account the spectral windows and flux points defined by BA86a and BA86b. Given the low spectral dispersion used, there exist several maximum flux points which allow the continuum of each spectrum to fit satisfactorily, even if the points are connected by straight lines. The flux points were fitted to the corresponding local Balmer continuum using the SPLINE/SPEED routine. We performed two additional fits using high and low continuum tracings in order to take into account the spectral noise in the measurements of the Balmer-line equivalent widths. The derived uncertainties are found to be smaller than those quoted by BA86b for the intrinsic Balmer-line dispersions. The mean ages derived from Hα to Hδ Balmer lines are listed, together with their estimated errors, in column (6) of Table 4.

The selection of template cluster spectra was performed considering the ages derived from the Balmer-line method. These template spectra, taken from Bica (1988), Bica, Alloin & Santos (1990) and Santos et al. (1995), are average spectra of Magellanic Cloud and Galactic star clusters grouped according to their evolutionary stages. The template groups useful in the present analysis are Y3B (age $t \approx 100$ Myr) and Y4 ($t \approx 500$ Myr), which cover the observed spectral range. Furthermore, we used the YEF ($t \approx 50$–110 Myr) and YG ($t \approx 110$–170 Myr) templates in the blue range, whereas YE ($t \approx 50$–85 Myr), YG ($t \approx 130$–250) and YH ($t \approx 250$–750 Myr) were taken into account in the red range. All these templates

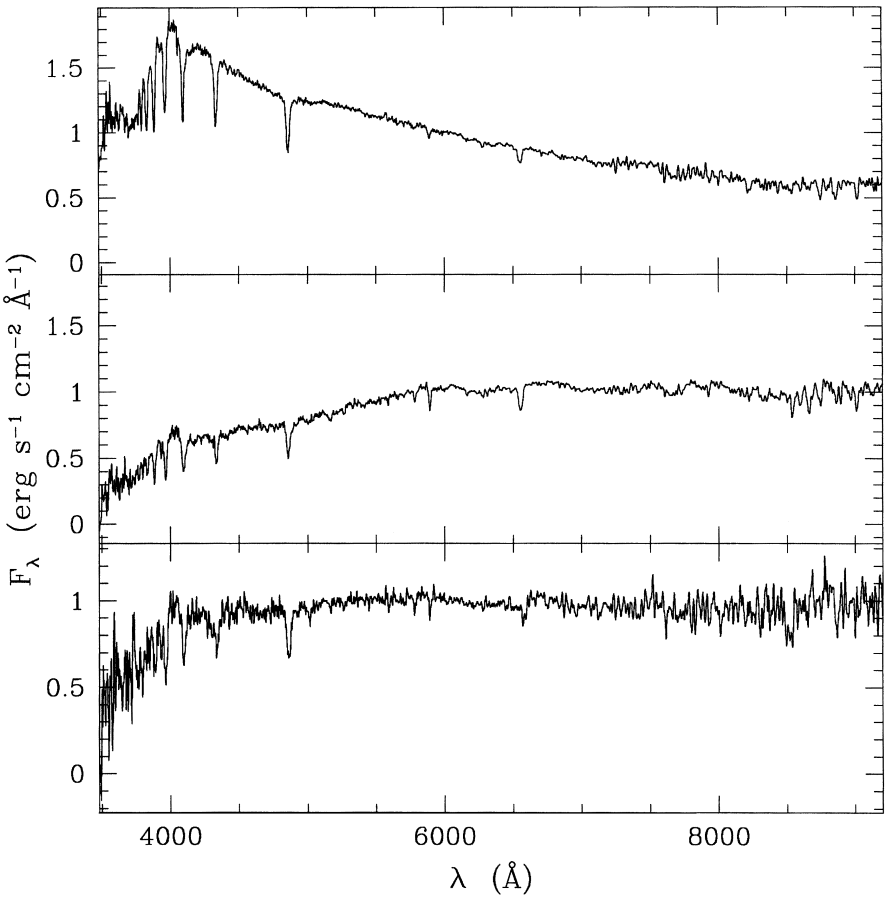

Figure 5. Observed integrated spectra in absolute F_λ unit: NGC 6031 (top), Ruprecht 115 (middle) and Ruprecht 120 (bottom).

Table 4. Cluster fundamental parameters derived from the spectroscopic analysis.

Cluster	W(Balmer) (Å)				Balmer age	Template age	$E(B-V)$
	H_α	H_β	H_γ	H_δ	(Myr)	(Myr)	
NGC 6031	5.85±0.29	8.61±0.26	8.94±0.44	9.90±0.49	250±100	100	0.15
Ruprecht 115	5.15±0.15	8.42±0.08	8.54±0.26	13.23±0.40	500±10	500	0.50
Ruprecht 120	7.20±0.07	8.36±0.18	7.76±0.31	10.34±0.21	100±10	100	0.55

were separated in age bins shorter than Y3B and Y4, but due to their small spectral range they were used only for control purposes. The reddening and age of the programme clusters were determined by varying the templates and $E(B-V)$ colour excesses to get the best match to both the continuum and lines of the cluster spectra. To perform reddening correction, we used the interstellar absorption law derived by Seaton (1979). The age of the template which most resembles the cluster spectrum and the resulting $E(B-V)$ colour excess are listed in columns (7) and (8) of Table 4. The uncertainty in the reddening estimation is typically ~ 0.05 dex.

Fig. 6 shows the observed integrated spectra of NGC 6031 and Ruprecht 120 corrected for the derived foreground reddening values. These spectra were normalized to $F_\lambda = 1$ at $\lambda = 6000$ Å, and shifted with an additional constant when necessary. As can be seen, the template Y3B successfully reproduces the continuum slope and intensities of the Balmer lines observed in the spectra of NGC 6031 and Ruprecht 120. It must be noted, however, that template spectra are the average of integrated spectra of several different clusters and, consequently, they represent the stellar population synthesis of clusters within a limited age range. Therefore small spectral differences between the observed spectra and the template ones can be expected. For example, the Balmer absorption discontinuty of Y3B appears to be slightly more pronounced than those in NGC 6031 and Ruprecht 120. However, these differences could also come from a decrease in the sensivity of our spectroscopic set-up towards the shortest wavelenghts. This is clearly visible from the smaller S/N ratios of the observed NGC 6031 and Ruprecht 120 spectra with respect to Y3B in the 3500–4000 Å range.

Fig. 7 shows the reddening-corrected spectrum of Ruprecht 115 as compared to the Y4 template. They are normalized to $F_\lambda = 1$ at $\lambda = 6000$ Å and shifted by different constants. Although the spectra resemble each other well, the integrated spectrum of Ruprecht 115 presents some features more visible than in Y4, such as TiO bands at λλ7000–7400 Å, λλ7600–7800 Å, λλ8200–8400 Å and λλ8450–8600 Å. These TiO bands could correspond to

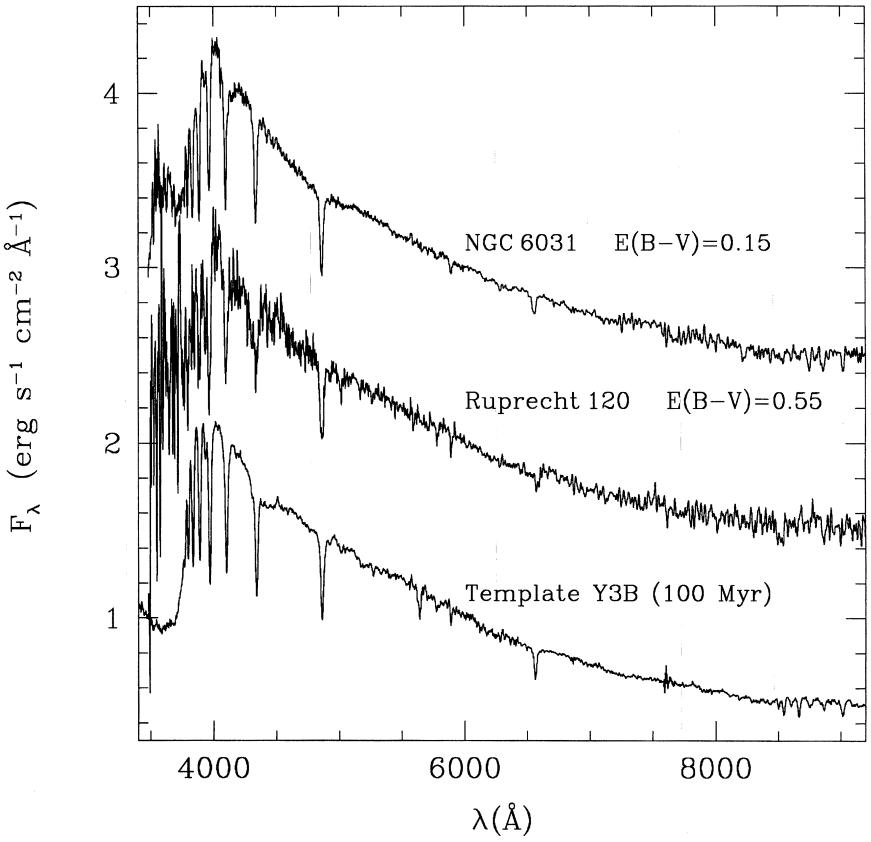

Figure 6. Reddening-corrected integrated spectra of NGC 6031 and Ruprecht 120 compared to the template Y3B.

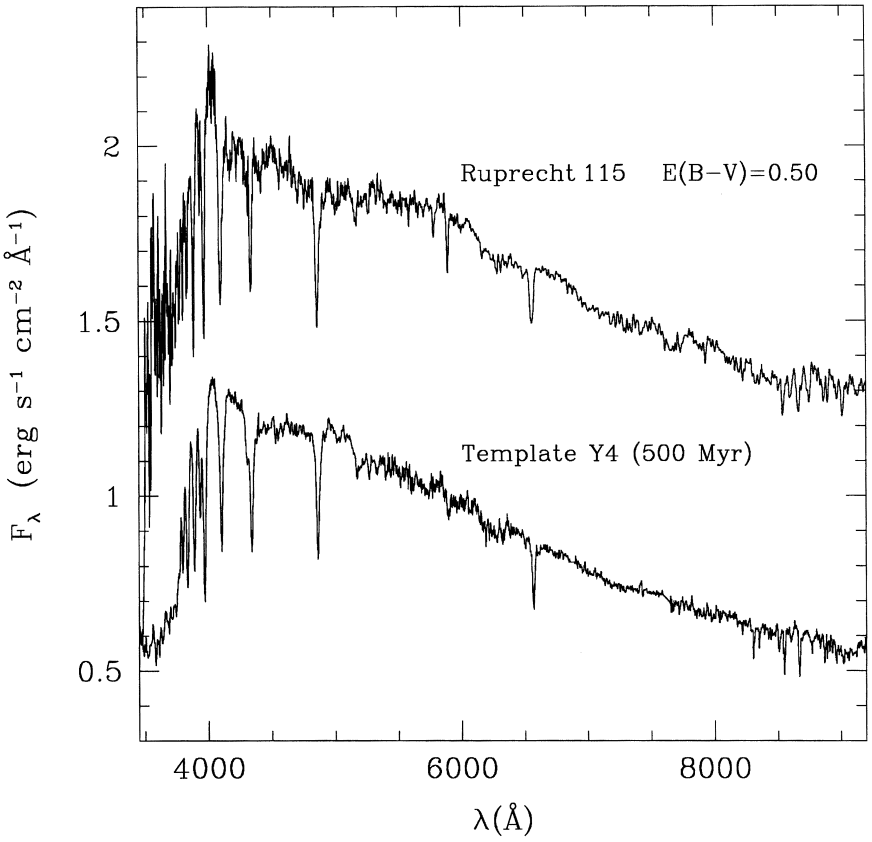

Figure 7. Reddening-corrected integrated spectrum of Ruprecht 115 compared to the template Y4.

Table 5. Equivalent widths (in Å) for the Ca II windows.

Window $\lambda_o/\Delta\lambda$ ident.	NGC 6031	Ruprecht 115	Ruprecht 120
8498/44 Ca II+P16	2.33±0.11	1.27±0.05	5.52±0.17
8542/44 Ca II+P15	3.14±0.06	4.53±0.02	4.27±0.16
8670/60 Ca II+P13	3.44±0.05	6.13±0.04	—

Table 6. Adopted cluster fundamental parameters.

Cluster	$E(B-V)$	$V_o - M_v$	d (kpc)	Age (Myr)	[Fe/H]
NGC 5999	0.45±0.05	11.7±0.4	2.2±0.4	400±100	0.18*
NGC 6031	0.40±0.15	11.6±0.7	2.1±0.7	200±100	0.0
Ruprecht 115	0.60±0.10	12.0±0.6	2.5±0.7	500±100	+0.2
Ruprecht 120	0.65±0.10	11.8±0.6	2.3±0.6	100±100	≥0.0

*Taken from Santos & Bica (1993).

the blue/red integrated colour transition possibly associated with the development of the giant branch (Renzini & Buzzoni 1986). In addition, the continuum of the integrated spectrum of Ruprecht 115 in the blue range appears to be slightly redder than that of the Y4 template.

The Ca II triplet at λ8498, λ8542 and λ8662 Å has proved to be very useful in deriving the metallicity of globular clusters from both individual giant and integrated light spectra (BA87; Geisler et al. 1995; Idiart, Thévenin & de Freitas Pacheco 1997). There are, however, some sources of scatter for open clusters younger than about 1 Gyr which affect the metallicity determinations based on their observed integrated spectra. These uncertainties are related to the different stellar components contributing to the integrated light rather than to errors arising from the quality of the spectrum itself. The contamination by TiO bands and Paschen lines affect the Ca II windows. TiO may reinforce the metallicity dependence of the Ca II triplet (especially for the 8498- and 8542-Å lines), while Paschen lines introduce a systematic increase of the equivalent widths for blue clusters whatever their metallicities are. The Paschen absorptions affect the Ca II 8662-Å line more.

In order to obtain a rough estimation of the metallicities of NGC 6031, Ruprecht 115 and Ruprecht 120, we first measured the equivalent widths (Ws) of the Ca II triplet lines using the regions around λλ8408 and 8700 Å (BA87) as continuum points. Unfortunately, we could not measure the Ca II 8662-Å line in Ruprecht 120 because of the relatively high telluric absorption band residuals. Table 5 presents the window limits and the Ws. The error assigned to each measurement was calculated by considering local high and low continuum tracings. Then we compared the sums of the W(Ca II) with those measured by BA87 and Santos & Bica (1993) for open clusters with independent metallicity determinations from individual stars. The sum of the three Ca II lines in NGC 6031 is $\Sigma W = 8.91 \pm 0.22$, which compares well with 8.8 and 9.6 of NGC 2660 and 6067, whose iron-to-hydrogen ratios are −0.02 (Janes 1979) and 0.01 (Luck 1994), respectively. For Ruprecht 115 we found $\Sigma W = 11.93 \pm 0.11$, which is slightly higher than 10.3 of NGC 6705 ([Fe/H] = +0.21, Thogersen, Friel & Fallon 1993). From this comparison, we conclude that NGC 6031 has nearly solar metal content, while Ruprecht 115 appears to be slightly metal-rich. Finally, the W-values of the two measured lines in Ruprecht 120 suggest that this cluster is slightly more metal-rich than the Sun.

3.3 Cluster parameters

The resulting photometric and spectroscopic fundamental parameters for the present cluster sample were combined in order to derive their final values (Table 6). The $E(B-V)$ colour excesses were averaged, assigning double weight to the photometric determinations. This criterion was adopted because the photometric $E(B-V)$ colour excess is a more reliable indicator of the mean total absorption affecting the cluster. Note that only foreground reddening has been applied to the templates spectra and, consequently, if a determination of total (foreground + internal) reddening is available, the internal reddening due to dust within the cluster may be estimated. In this sense, the comparatively large difference between the photometric and spectroscopic reddening values for NGC 6031 could be indicating the existence of internal reddening affecting this cluster. For the remaining clusters both reddening determinations show reasonably good agreement. In the case of NGC 5999, we adopted the results provided by the photometric analysis. The true distance moduli and hence the cluster distances were calculated from the adopted $E(B-V)$ colour excesses and apparent distance moduli listed in Table 3. The errors in the distance determinations were calculated, taking into account the uncertainties in the $E(B-V)$ colour excess and apparent distance modulus through the expression $\sigma(d) = 0.46\ \{\sigma(V-M_v) + 3\sigma[E(B-V)]\}d$, where $\sigma(V-M_v)$ and $\sigma[E(B-V)]$ represent the estimated errors in $V-M_v$ and $E(B-V)$. The adopted cluster ages were obtained by averaging the three independent estimates, namely the age obtained from the isochrone-fitting, the age derived from the Balmer-line method and that of the template spectrum used to derive cluster reddening. All these agree well.

NGC 6031 has been previously studied by different authors, who placed it approximately between 1.0 and 3.0 kpc from the Sun (Lindoff 1967; MV75; Topaktas 1981), regardless of old cataloguing works which set this value from 1.7 through to 7.7 kpc. Though our cluster distance is nearly the average between 1.0 and 3.0 kpc, only Topaktas's distance estimation ($d = 1.6$ kpc) is within an error bar of $1\sigma(d)$. We therefore believe that we have improved our knowledge about the distance of NGC 6031. The adopted $E(B-V)$ colour excess (0.40 ± 0.15) shows very good agreement with the values of 0.43, 0.47 and 0.46 derived by Lindoff (1967), MV75 and Topaktas (1981), respectively. However, the comparatively large difference between our phtometric and spectroscopic colour excesses could be indicating that the cluster is affected by internal reddening. Though moderately young, NGC 6031 appears to be 3 times older than the age derived by Lindoff (1967).

NGC 5999 has only spectrocopic data available. Santos & Bica (1993) obtained an integrated spectrum of the cluster and derived a foreground reddening of $E(B-V) = 0.44$ and an age of 200 ± 150 Myr. Their $E(B-V)$ colour excess is nearly the same as we derive in this study, but their estimated age is somewhat smaller than ours. In spite of the considerable uncertainties affecting both age estimations, the mean ages still remain distinguishable.

4 CONCLUSIONS

CCD *BVI* Johnson–Cousins photometry of stars in the fields of the poorly studied or unstudied southern open clusters NGC 5999,

NGC 6031, Ruprecht 115 and Ruprecht 120 is presented. We have also carried out *BV* photoelectric measurements of 27 bright stars in the field of NGC 5999. The photoelectric data allowed us not only to observe the bright end of the cluster sequence, but also to test the quality of the CCD photometry. The present photometric data of NGC 6031 supersede previous ones by MV75 and Topaktas (1981), thus allowing us to extend the corresponding MS 3 mag fainter.

From the observed CMDs we confirmed that NGC 5999, NGC 6031, Ruprecht 115 and Ruprecht 120 are genuine open clusters and identified the most important features of the cluster HR diagrams, including their main sequences and turn-off points. We also recognized the contribution of different disc star populations in the field of Ruprecht 115. Reddenings, distances and ages were derived for the four clusters.

Integrated spectra for NGC 6031, Ruprecht 115 and Ruprecht 120 covering a range from 3500 to 9200 Å are also presented. From the Balmer-line equivalent widths and the matching of template spectra on the observed ones, we derived reddening and age. Cluster metallicities have also been estimated from the equivalent widths of the infrared Ca II triplet.

The photometric and spectroscopic results indicate that NGC 5999, NGC 6031, Ruprecht 115 and Ruprecht 120 are moderately young open clusters, with ages ranging from 100 to 500 Myr. The four clusters are located approximately towards the Galactic Centre at a distance of ~ 2.3 kpc from the Sun, and are all affected by $E(B-V) \sim 0.5$. Their metallicities range between typical values of solar to moderately metal-rich open clusters. By increasing the sample of open clusters with well-known metallicities, ages and positions, especially those located in the direction of the Galactic Centre, we will be able to improve the knowledge of the chemical evolution of the disc of our Galaxy (Piatti, Claria & Abadi 1995; Twarog, Ashman & Anthony-Twarog 1997).

ACKNOWLEDGMENTS

We are grateful for the use of the CCD and data acquisition system at CASLEO supported by US National Science Foundation grant AST-90-15827. We also thank Las Campanas staff for their kind hospitality and assistance during the observing runs, and the Vitae and Antorchas Foundations for their help. We are indebted to M. A. Nicotra for helping us with the software support. This work has been financially supported by the institutions CONICOR and CONICET (Argentina) and CNPq and FINEP (Brazil).

REFERENCES

Barkhatova K. A., 1960, Z. Astrophys., 51, 49
Bica E., 1988, A&A, 195, 76
Bica E., Alloin D., 1986a, A&A, 162, 21 (BA86a)
Bica E., Alloin D., 1986b, A&AS, 66, 171 (BA86b)
Bica E., Alloin D., 1987, A&A, 186, 49 (BA87)
Bica E., Alloin D., Santos J. F. C., Jr, 1990, A&A, 235, 103
Bica E., Clariá J. J., Bonatto Ch., Piatti A. E., Ortolani S., Barbuy B., 1995, A&A, 303, 747
Bica E., Clariá J. J., Piatti A. E., Bonatto C., 1998, A&AS, 131, 483
Burki G., Maeder A., 1973, A&A, 25, 71
Clariá J. J., Lapasset E., 1991, PASP, 103, 998
Collinder P., 1931, Annals of the Observatory of Lund No. 2
Daniel S. A., Latham D. W., Mathieu R. D., Twarog B. A., 1994, PASP, 106, 281
Fenkart R., Binggeli B., 1979, A&AS, 35, 271
Geisler D., Piatti A. E., Clariá J. J., Minniti D., 1995, AJ, 109, 605
Graham J. A., 1982, PASP, 94, 244
Gutiérrez-Moreno A., Moreno H., Cortés G., Wenderoth E., 1988, PASP, 100, 973
Hawarden T. G., 1974, MNRAS, 169, 539
Idiart T. P., Thévenin F., de Freitas Pacheco J. A., 1997, AJ, 113, 1066
Janes K. A., 1979, ApJS, 39, 135
Janes K. A., Phelps R. L., 1990, in Philip A. G. D., ed., CCDs in Astronomy II. David Press, Schenectady, p. 117
Kassis M., Friel E. D., Phelps R. L., 1996, AJ, 111, 820
Landolt A. U., 1973, AJ, 78, 959
Landolt A. U., 1992, AJ, 104, 340
Lindoff U., 1967, Ark. Astron., 4, 305
Luck R. E., 1994, ApJS, 91, 309
Meynet G., Mermilliod J. C., Maeder A., 1993, A&AS, 98, 477
Moffat A. F. J., Vogt N., 1975, A&AS, 20, 155 (MV75)
Montgomery K. A., Marschall L. A., Janes K. A., 1993, AJ, 106, 181
Ng Y. K., Bertelli G., Chiosi C., Bressan A., 1996, A&A, 310, 771
Piatti A. E., 1996, Thesis Doctoral, Universidad Nacional de Córdoba
Piatti A. E., Clariá J. J., Abadi M. G., 1995, AJ, 110, 2813
Piatti A. E., Bica E., Clariá J. J., 1998a, A&AS, 127, 423
Piatti A. E., Clariá J. J., Bica E., Geisler D., Minniti D., 1998b, AJ, 116, 801
Piatti A. E., Clariá J. J., Bica E., 1998c, ApJS, 116, 263
Renzini A., Buzzoni A., 1986, in Chiosi C., Renzini A., eds, Spectral Evolution of Galaxies. Reidel, Dordrecht p. 135
Rosvick J. M., 1995, MNRAS, 277, 1379
Santos J. F. C., Jr., Bica E., 1993, MNRAS, 260, 915
Santos J. F. C., Jr., Bica E., Clariá J. J., Piatti A. E., Girardi L. A., Dottori H., 1995, MNRAS, 276, 1155
Schmidt A., 1988 User Manual, Federal University of Santa María (Brazil)
Schmidt-Kaler Th., 1982, in Schaifers K., Voigt H. H., eds, Landolt-Börnstein. Numerical Data and Functional Relationships in Science and Technology, New Series, group VI, Vol. 2b. Springer Verlag, Berlin
Seaton M. J., 1979, MNRAS, 187, 73
Stetson P. B., 1991, DAOPHOT User Manual
Stone R. P. S., Baldwin J. A., 1983, MNRAS, 204, 347
Straižys V., 1990, Multicolor Stellar Photometry. Pachart Publ. House, Tucson, Arizona
Thogersen E. N., Friel E. D., Fallon B. V., 1993, PASP, 105, 1253
Topaktas L., 1981, A&AS, 45, 111
Trumpler R. J., 1930, Lick Obs. Bull., 14, 154
Turner D. G., 1976, AJ, 81, 1125
Twarog B. A., Ashman K. M., Anthony-Twarog B. J., 1997, AJ, 114, 2556
Vázquez R. A., Baume G., Feinstein A., Prado P., 1996, A&AS, 116, 75
Walker A. R., 1985, MNRAS, 213, 889

This paper has been typeset from a TEX/LATEX file prepared by the author.